Studies on the evolution of alkali silicate in a simulated alkali-silica reaction system

ZHENG Kunpeng[1, a*], ADRIAENSENS Peter[2, b], DE SCHUTTER Geert[1, c], YE Guang[1, 3, d], TAERWE Luc[1, e]

[1]Magnel Laboratory for Concrete Research, Department of Structural Engineering, Ghent University, Ghent 9052, Belgium

[2]Applied and Analytical Chemistry, Institute for Materials Research, University of Hasselt, Hasselt 3590, Belgium

[3]Microlab, Faculty of Civil Engineering and Geosciences, Delft University of Technology, Delft 2628 CN, The Netherlands

[a] kunpeng.zheng@ugent.be, [b] peter.adriaensens@uhasselt.be, [c] geert.deschutter@ugent.be, [d] g.ye@tudelft.nl, [e] luc.taerwe@UGent.be

*corresponding author

Keywords: alkali-silica reaction; alkali silicate; chemical model system; evolution.

Abstract

In this study, the interaction between the reactive silica present in aggregates and the alkalis and hydroxyls present in the pore solution of cement paste is simulated in a chemical model system and investigated experimentally. Various properties of the solid and liquid phases are investigated. The results show that the nano and micro structure and properties of the formed alkali silicate change significantly during this process.

1. Introduction

Alkali-silica reaction (ASR), since it was firstly reported in 1940 [1], is one of the most serious durability problems of concrete leading to deterioration. The process of ASR consists a series of physico-chemical reactions between the reactive silica contained in the aggregates and the multiple components present in the cement paste leading to the formation of ASR gel. Considering the decisive effect of ASR gel on the consequent deterioration, the investigation on this topic is of great importance to improve our understanding about the mechanism of ASR.

Although the term “ASR gel” is widely used for representing the products responsible for the expansion and cracking caused by ASR, it does not give any information about the intrinsic properties of those products leading to a possible underestimation about the complexity of the related processes. In the light of this consideration, it is necessary to clarify the definition of ASR gel by following its formation processes.

Generally speaking, ASR gel can be classified into two types concerning whether it contains calcium or not: alkali silicate and calcium alkali silicate.

Once the reactive silica contained in the aggregates comes into contact with the pore solution, the Si-O-Si bonds (siloxanes) on the surface of silica are destroyed by those hydroxyls to generate Si-OH bonds (silanols) [2] leading to a local hydrolysis as stated by Brinker [3], see Eq. 1. As a consequence, the influenced silicon-oxygen network on the surface of silica is modified from a relatively closed structure to a more open and dis-organized one. If OH^- is sufficiently provided by the pore solution, more siloxanes can be attacked by OH^- resulting in further hydrolysis. This eventually causes the destruction of the affected silicon-oxygen network.

$$2OH^- + (\equiv Si\text{-}O\text{-}Si\equiv) \rightarrow 2(\equiv Si\text{-}O)^- + H_2O. \quad (1)$$

The formed silicate is negatively charged, therefore it can be neutralized by the alkalis (Na^+ and K^+) present in the pore solution. As a result, the alkalis are incorporated into the silicon-oxygen network, i.e. alkali silicate is formed. This process is shown in Eq. 2 where R denotes the alkalis including Na^+ and K^+, where O…R means the bond between oxygen and alkali is like a strong Van der Waals force [4].

$$(\equiv Si\text{-}O)^- + R+ \rightarrow \equiv Si\text{-}O\ldots R. \quad (2)$$

Due to the minimum energy variation between different alkali silicates [5], the formed alkali silicates can interlink with each other to form a more complex type of alkali silicate with larger size and higher polymerization degree [6]. This process is known as condensation or polymerization shown in Eq. 3 [7]. As a consequence, a new and more cross-linked silicon-oxygen network is formed [8, 9]. Many studies [8, 10, 11] suggested that a higher concentration of silicate, a lower pH value and a longer reaction time favored the polymerization.

$$-SiOH + HOSi- \rightarrow -SiOSi- + H_2O. \quad (3)$$

If calcium is present in this system in the form of either Ca^{2+} or $Ca(OH)_2$, it can get incorporated into the silicon-oxygen network to form calcium alkali silicate by Eq. 4 [12]. Since the incorporation of calcium happens after the hydrolysis of silica, this process can be considered as the interaction between alkali silicate and calcium.

$$Ca^{2+} + 2(\equiv Si\text{-}O)^- \rightarrow (\equiv Si\text{-}O\ldots Ca\ldots O\text{-}Si\equiv). \quad (4)$$

Compared to the formation of alkali silicate (Eq. 1 and Eq. 2) which is well studied and closely related to ASR [13-15], the influence of the evolution of alkali silicate (Eq. 3) on ASR draws little attention [16], though it does have a significant effect on changing the nano and micro structure of alkali silicate and consequently modifying its properties and the performance when it interacts with calcium in the subsequent reaction (Eq. 4). This study was carried out in view of this consideration.

2. Materials and Method

In this study, silica fume (Elekem Microsilica Grade 940U, Oslo, Norway) was chosen as the silica source to simulate the reactive silica contained in the aggregates. The composition of the silica fume in the form of oxides is given in Table 1, and the X-ray diffraction (XRD) pattern of the used silica fume is shown in Fig. 1. To simulate the pore solution of the cement paste, the NaOH solution with a concentration of 1 mol/L was obtained by dissolving pellets of NaOH in deionized and CO_2-free water.

Table 1: Chemical composition of the silica fume [wt %].

Compositions	SiO_2	CaO	Al_2O_3	Fe_2O_3	MgO	Na_2O	K_2O	SO_3
Content	94.2	0.6	1.0	0.5	0.7	1.0	1.1	0.3

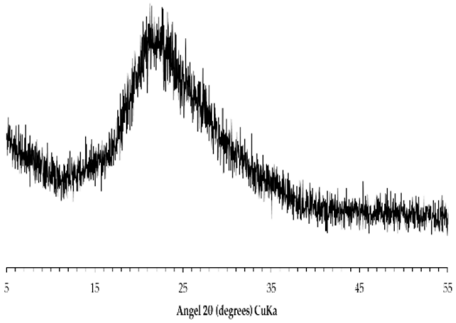

Fig. 1: XRD pattern of silica fume used in this study.

The interaction between silica fume and 1 mol/L NaOH solution is used for simulating the first step of ASR where the reactive silica in aggregates interacts with the pore solution of cement paste to form alkali silicate. (1) Add 1 mol/L NaOH solution to the silica fume at a liquid to solid mass ratio of 3 to ensure sufficient silica for the partial silica dissolution [17] similar to the situation in ASR [6]; (2) seal the mixture of 1mol/L NaOH solution and silica fume in a polypropylene bottle which was filled with N_2 to prevent contamination; (3) mix the mixture with a rotary mixer at a speed of 60 rpm at room temperature; (4) stop the mixing after the desired mixing time for sample collection.

After the desired mixing time (0 hour, 1 hour, 6 hours, 12 hours, 18 hours, 24 hours and 48 hours), the mixture was poured into a container filled with isopropanol to cease any further reactions by removing the water in the system. The immersion period lasted for 24 hours. In order to ensure a considerable efficiency for this step, the volume ratio of isopropanol to the alkali silicate slurry was about 100. After the desired immersion time, the residue was obtained by filtering with vacuum. In the end, the residue was vacuum dried for 4 days until it was ready for analysis.

The alkali silicate slurries mixed for 0 hour, 1 hour, 6 hours, 12 hours, 18 hours, 24 hours and 48 hours were collected for the analysis of the concentration of silicon and hydroxyl.

Notably, the conventional method of acquiring solution from slurry by filtering several times is time-consuming and prone to contamination. Accordingly, a method combining centrifuge and filtering was designed. (1) The mixture was poured into the container for centrifuge at 3000 rpm for 3 minutes; (2) the liquid layer located at the top was filtered twice through filter papers with particle retention of 12-15 µm first and 2 µm in sequence to get a clear solution for further analysis. This procedure was carried out in the glove box filled with N_2; (3) the acquired solution was distributed evenly into two parts to analyze the concentrations of silicon and hydroxyl, respectively. (4) the samples were stored in a fridge at a temperature of 5 °C for 3 hours at most, until their analysis.

In order to evaluate the quantity of hydroxyl groups (-OH) in alkali silicate, an acid-thermal treatment proposed originally by Bulteel et al. [18] was followed with minor modification. In this method, H^+ from HCl firstly neutralizes the access OH^- in the slurry and secondly exchanges with the incorporated alkalis in alkali silicate. This results in the protonation of alkali silicate to form silanols and/or silicic acid. The newly formed hydroxyl groups can be removed as water vapor during the thermal treatment. The volume ratio of the HCl solution to the alkali silicate slurry was set as about 100 to ensure the efficiency of protonation. The steps are given as follows: (1) 40 g of alkali silicate slurry was poured into a container with a 0.5 mol/L of HCl solution; (2) the mixture of alkali silicate slurry and HCl solution was mixed with a magnetic stirrer for 1 hour at room temperature; (3) the mixture was filtered with vacuum; (4) the residue was dried under vacuum for 4 days under room temperature; (5) the sample was heated up to 1000 °C in an oven.

The quantity of hydroxyl group in alkali silicate can be calculated based on the mass difference before and after the thermal treatment. The calculation is given in Eq. 5, where m_0 denotes the mass of the sample before the thermal treatment in the unite of gram (g); m_t denotes the mass of the sample after thermal treatment (g); M_{H2O} denotes the molar mass of water (g/mol).

Molarity of hydroxyl group per gram = $\frac{m_0 - m_t}{M_{H2O} \times m_0}$. (5)

The concentrations of silicon in the system at different reaction times were measured with an Inductively Coupled Plasma coupled with Optical Emission Spectrometry (ICP-OES). The concentration of OH^- remaining in solution can be calculated from the pH level measured with a pH meter in a glove box filled with N_2. The waiting time for the stabilization of the display was not more than 2 minutes for each measurement.

The specific surface area (SSA) of the solid product was measured with the nitrogen absorption method following the Brunauer-Emmett-Teller (BET) model with VacPrep 061 for the pre-vacuum treatment and TriStar 3000 for the measurement.

^{29}Si solid-state cross-polarization (CP)/Magic angle spinning (MAS) nuclear magnetic resonance (NMR) spectra were acquired to obtain the information about the silicon-oxygen networks present in the system [19].

3. Results and Discussion

3.1 pH Level and Concentration of Silicon. The concentrations of silicon and hydroxyl during the interaction between silica fume and NaOH solution were measured with ICP-OES and pH meter, respectively. The results are given in Fig. 2.

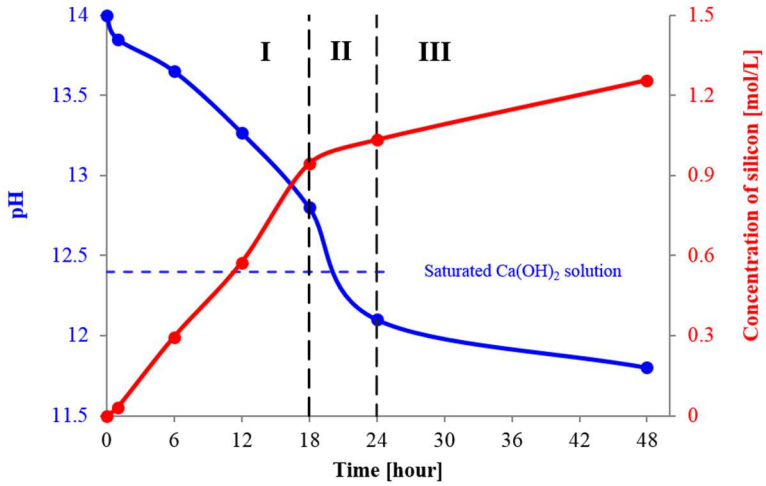

Fig. 2: pH level and concentration of silicon.

As shown in Fig. 2, the pH level of the solution declines significantly in the first 24 hours. This is caused by the consumption of OH^- which attacks the siloxanes and destroys the tetrahedral network of silica. From 24h to 48h, the decrease of pH slows down. In particular, the pH level is about 12.2 (concentration of OH^- ($[OH^-]$) is 0.016 mol/L) at 24h; the pH level is 11.8 ($[OH^-]$=0.006 mol/L) at 48h. Considering the concentration of OH^- provided by the NaOH solution was 1 mol/L at the beginning, most OH^- (98%) present in the solution has been reacted in the first 24 hours. If $Ca(OH)_2$ is present in this solution and the interaction between alkali silicate and calcium is ignored, the pH level at about 19h is low enough to trigger the dissolution of $Ca(OH)_2$ to release Ca^{2+} and OH^-, since the pH value of the system is lower than that of a saturation solution of $Ca(OH)_2$ (pH=12.4).

The concentration of silicon measured by ICP-OES represents the concentration of the dissolved alkali silicate in the solution. The concentration of silicon increases significantly in the beginning and reaches a value of about 0.94 mol/L at 18h. From then on, the concentration of silicon experiences a slower increase to 1.03 mol/L at 24h and eventually 1.25 mol/L at 48h. This indicates that most dissolved alkali silicate is formed and released into the solution in the first 18 hours. This is consistent with the results of the pH level, showing that a large amount of dissolved alkali silicate is released by the interaction between the silica fume and the NaOH solution. From 18h to 24h (Zone II), the

increase of the concentration of silicon slows down indicating that the dissolved alkali silicate might approach its saturation. The pH level continues to decrease in the meantime suggesting a continuous consumption of OH^- during this period. This consumption is likely caused by both the limited interaction between OH^- and silica fume to form alkali silicate and the interaction between OH^- and the existing alkali silicate. Considering the minor increase of the concentration of silicon resulting from the formation of alkali silicate which newly enters the solution, the considerable decrease of the pH level during this period can be mainly attributed to the interaction between OH^- and the existing dissolved alkali silicate. From 24h to 48h (Zone III), the concentration of silicon and pH level experience little change suggesting the system is almost at an equilibrium at this moment.

3.2 Silicon-oxygen Network. In order to characterize the evolution of the silicon-oxygen network, NMR tests were carried out. It is necessary to introduce the standard notation of Q^n nomenclature to interpret the NMR spectra [20]. Q represents a given tetrahedron; the exponent n represents the number of associated bridges of oxygen with silicon. In this way, a Q^4 tetrahedron has four oxygen bridges with silicon suggesting the existence of a complete interlinked silicon-oxygen organization, e.g. a 3D structure. A Q^3 tetrahedron has three bridging oxygens and one non-bridging oxygen suggesting this tetrahedron has one bond available for bridging. Notably, the non-bridging oxygen can be bonded to another cation other than silicon, e.g. bonded to a proton to form an –OH group. A Q^2 tetrahedron has two bridging oxygens and two non-bridging oxygens indicating the existence of a less cross-linked silicon-oxygen network compared to Q^3. Q^2 is usually found to be present as part of a chain. A Q^1 tetrahedron has only one bridging oxygen with silicon and three non-bridging oxygens, which is usually found to be present at the end of a structure. Q^0 tetrahedron has four non-bridging oxygens and is usually present as monomer $Si(OH)_4$.

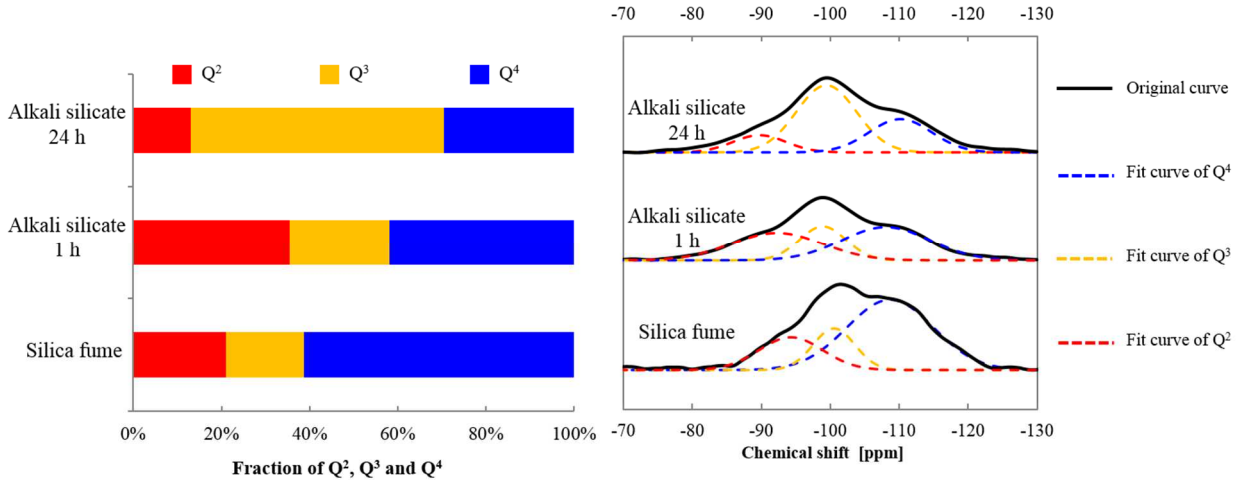

Fig. 3: ^{29}Si NMR results of the silicon-oxygen networks in alkali silicate slurry with different reaction times.

As shown in Fig. 3, the silica fume contains Q^2, Q^3 and Q^4. In particular, the fraction of Q^4 is more than 60%, the fraction of Q^2 is about 21% and that of Q^3 is about 17%. This suggests the silica fume is mainly composed of the fully cross-interlinked silicon-oxygen network (Q^4) with some other species of Q^3 and Q^2.

For the sample collected from the alkali silicate slurry after 1 hour of reaction, its NMR spectrum shifts downfield (the left) compared to that of silica fume indicating an ongoing de-polymerization featured by an increasing amount of Q^2 and Q^3 at the expense of Q^4. In particular, the fraction of Q^4 decreases from more than 60% in the silica fume to about 40% at 1h; the fraction of Q^3 increases from about 17% in the silica fume to about 23%; the fraction of Q^2 increases from about 21% in the silica fume to about 36%. Obviously, during this process, a large number of Q^4 (or even part of Q^3) are attacked by OH^- to generate Q^2 leading to the formation of a less cross-linked silicon-oxygen network. As a result, the silicon-oxygen network is destroyed. Notably, Q^4 here could represent the unreacted silica fume present in the system.

For the sample collected from the alkali silicate slurry after 24 hours of reaction, the fraction of Q^4 decreases from about 40% to about 29%; the fraction of Q^3 increases significantly from about 23% to about 57%; the fraction of Q^2 decreases from 36% to about 13%. The decrease of the fraction of Q^4 confirms the ongoing de-polymerization process during which Q^4 is decomposed. The increase of the fraction of Q^3 can be caused by two effects: the de-polymerization of Q^4 and the polymerization of Q^2 [7]. Similarly, the decrease of the fraction of Q^2 can also be attributed to two processes: the de-polymerization of Q^2 to form Q^1 or Q^0, the polymerization of Q^2 to form Q^3. The processes of de-polymerization and polymerization are schematically illustrated in Fig. 4. However, the featured peaks assigned to Q^1 and Q^0 cannot be found in Fig. 3. Therefore, the decrease of the fraction of Q^2 is caused by its polymerization to form Q^3. This conclusion is consistent with the results given in Fig. 2, indicating that a low value of pH benefits the occurrence of polymerization [10]. In this sense, it is clear that the silicon-oxygen network present in the system at 24h is experiencing both de-polymerization and polymerization making it more complex and cross-linked compared to that from the system at 1h [8, 9, 21].

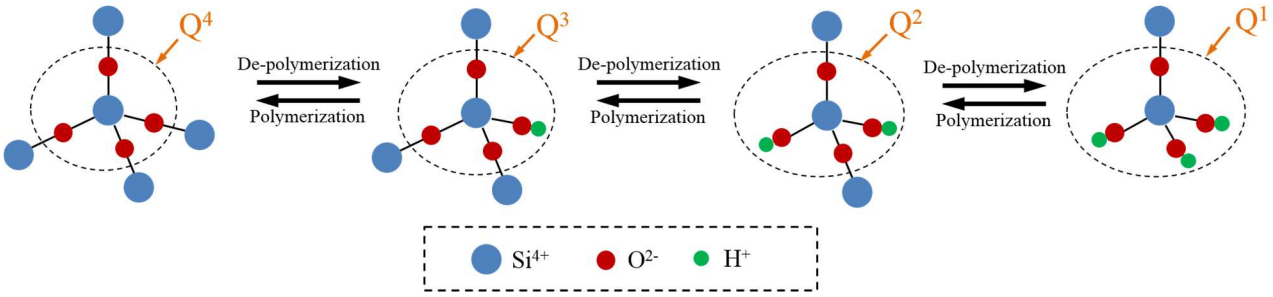

Fig. 4: Schematic representation of de-polymerization and polymerization.

De-polymerization and polymerization occur during the interaction between the silica fume and the NaOH solution. The de-polymerization predominates the silicon-oxygen network at the early age while the polymerization is stimulated at the latter time. During de-polymerization, OH^- as well as alkalis from solution attacks the siloxanes contained in the silicon-oxygen network of silica fume leading to the destruction of the network. As a result, the polymerization degree decreases.

At the later age, the increase of concentration of alkali silicate in the system as well as the decreased pH level stimulates polymerization [8]. During polymerization, the silanols tend to interlink with each other to generate siloxanes forming a more complex and dis-ordered silicon-oxygen network. As a result, the polymerization degree of the alkali silicate increases. It should be clarified that, the original silicon-oxygen network is destroyed during de-polymerization to form smaller species. During polymerization, those smaller species interlink with each other to construct a new silicon-oxygen network. Therefore, the de-polymerization and polymerization here are never a pair of reversible processes. The silicon-oxygen network formed from polymerization has a more complex and dis-organized structure compared to the original one.

To summarize, during de-polymerization, hydroxyls and alkalis destroy the original silicon-oxygen network of silica fume leading to the formation of alkali silicate with a decreased polymerization degree at the early age. As polymerization is stimulated, a more complex and dis-ordered silicon-oxygen network is generated by the re-construction of siloxane bonds at the later age. In addition, those changes on the silicon-oxygen network of alkali silicate will inevitably affect the interaction between alkali silicate and calcium (Eq. 4).

3.3 Specific Surface Area (SSA_{BET}) and hydroxyl Groups. During the interaction between the silica fume and the NaOH solution, the specific surface area (SSA_{BET}) and the quantity of the hydroxyl group contained in silicon-oxygen network will change accordingly. The results are shown in Fig. 5.

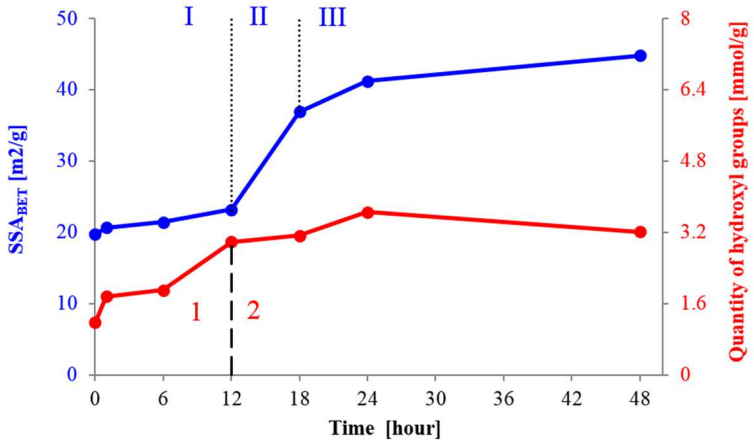

Fig. 5: SSA_{BET} and content of hydroxyl group.

As shown in Fig. 5, SSA_{BET} increases with time. In the first 12 hours (Zone I), it slightly increases from about 19 m^2/g to about 23 m^2/g. In the next 6 hours from 12h to 18h (Zone II), SSA_{BET} increases significantly to about 37 m^2/g. From 18h to 48h (Zone III), SSA_{BET} slightly increases to about 44 m^2/g. Apparently, more surface areas accessible for N_2 are generated during the interaction between the silica fume and the NaOH solution. It is possible that the attack of OH^- destroys the silicon-oxygen network generating a structure which is more accessible for N_2. In the first 12 hours, the slight increase of SSA_{BET} is probably due to the limited contact of the siloxanes with the hydroxyls. Because the original silicon-oxygen network is probably able to protect the siloxane bonds located in the interior of the network from the attack of OH^- limiting the increase of the SSA_{BET}. As the reactions proceed progressively, more and more siloxane bonds are destroyed. As a result, the network gets more and more open resulting in the exposure of more siloxane bonds which are originally located at the interior, to the attack of OH^-. This leads to a significant increase of SSA_{BET}. In the end, due to the decreased concentration of OH^-, the attack of OH^- on the silicon-oxygen network slows down leading to the slight increase of SSA_{BET}.

The quantity of hydroxyl group contained in the silicon-oxygen network undergoes a similar but less significant increase during this process, compared to the SSA_{BET}. As indicated in Fig. 5, in the first 12 hours (Zone 1), the quantity of hydroxyl group increases notably from 1.17 mmol/g to 2.98 mmol/g. From 12h to 48h (Zone 2), it increases slightly from 2.98 mmol/g to 3.20 mmol/g. This is generally consistent with the results of SSA_{BET}.

It should be noted that, the hydroxyl group is mainly generated by the destruction of siloxanes to form silanols during de-polymerization; while be eliminated by the condensation of siloxanes during polymerization. It means that the quantity of hydroxyl group contained in the silicon-oxygen network is largely influenced by the factors affecting de-polymerization and polymerization processes.

Moreover, the amount of hydroxyl group in the alkali silicate has a critical effect in the subsequent interaction between alkali silicate and calcium given in Eq. 5. Hence, the alkali silicate having 1 hour of reaction time is expected to have a complete different performance during its interaction with calcium compared to the one having 24 hours of reaction time. This topic will be addressed in the further research.

4. Summary

In this study, the interaction between the silica fume and the NaOH solution is used for simulating the interaction between the reactive silica contained in the aggregates and the pore solution of cement paste. The concentrations of OH^- and silicon in solution were measured with a pH meter and ICP-OES, respectively. The change of the silicon-oxygen network during this process was investigated with ^{29}Si NMR. The changes of the specific surface area of the solid product and the content of hydroxyl groups contained in the solid product were analyzed as well.

Based on the above results and discussion, the following concluding remarks can be made:

- During the interaction between the silica fume and 1 mol/L of NaOH solution, the specific surface area of the solid product and the quantity of the hydroxyl group contained in the solid phase increase accordingly; the concentration of silicon in the solution increases, while the concentration of OH^- decreases.
- During the de-polymerization process at the early age, the alkalis and hydroxyls decompose the siloxanes in the silicon-oxygen network leading to the destruction of the network. As a result, a less cross-linked silicon-oxygen network is formed.
- Polymerization is triggered at the later age. As a result, a more complex and dis-ordered silicon-oxygen network is generated.

References

[1] T.E. Stanton, Expansion of concrete through reaction between cement and aggregate, ASCE Proceedings, 66 (1940) 1781-1811.

[2] R.K. Iler, The chemistry of silica: solubility, polymerization, colloid and surface pro perties, and biochemistry, Wiley-Interscience 1979.

[3] C. Brinker, Hydrolysis and condensation of silicates: effects on structure, Journal of Non-Crystalline Solids, 100 (1988) 31-50.

[4] F. Rajabipour, E. Giannini, C. Dunant, J.H. Ideker, M.D. Thomas, Alkali–silica reaction: Current understanding of the reaction mechanisms and the knowledge gaps, Cement and Concrete Research, 76 (2015) 130-146.

[5] A. Navrotsky, Physics and chemistry of Earth materials, Cambridge University Press, 1994.

[6] P.W. Wijnen, T.P. Beelen, K.P. Rummens, H.C. Saeijs, J.W. De Haan, L.J. Van De Ven, R.A. Van Santen, The molecular basis of aging of aqueous silica gel, Journal of Colloid and Interface Science, 145 (1991) 17-32.

[7] S.A. Greenberg, D. Sinclair, The polymerization of silicic acid, The Journal of Physical Chemistry, 59 (1955) 435-440.

[8] L.S.D. Glasser, E.E. Lachowski, G.G. Cameron, Studies on sodium silicate solutions by the method of trimethylsilylation, Journal of Applied Chemistry and Biotechnology, 27 (1977) 39-47.

[9] I.L. Svensson, S. Sjöberg, L.-O. Öhman, Polysilicate equilibria in concentrated sodium silicate solutions, Journal of the Chemical Society, Faraday Transactions 1: Physical Chemistry in Condensed Phases, 82 (1986) 3635-3646.

[10] S.D. Kinrade, T.W. Swaddle, Silicon-29 NMR studies of aqueous silicate solutions. 1. Chemical shifts and equilibria, Inorganic Chemistry, 27 (1988) 4253-4259.

[11] P. Wijnen, T. Beelen, J. De Haan, C. Rummens, L. Van de Ven, R. Van Santen, Silica gel dissolution in aqueous alkali metal hydroxides studied by 29Si-NMR, Journal of Non-Crystalline Solids, 109 (1989) 85-94.

[12] P. Nieto, R. Dron, R. Thouvenot, H. Zanni, F. Brivot, Study by 43 Ca NMR spectroscopy of the sol-gel transformation of the calcium-silicate complex, Comptes Rendus De L Academie Des Sciences Series II, 320 (1995) 485-488.

[13] E. Garcia-Diaz, J. Riche, D. Bulteel, C. Vernet, Mechanism of damage for the alkali–silica reaction, Cement and Concrete Research, 36 (2006) 395-400.

[14] M. Alnaggar, G. Cusatis, G.D. Luzio, Lattice Discrete Particle Modeling (LDPM) of Alkali Silica Reaction (ASR) deterioration of concrete structures, Cement and Concrete Composites, 41 (2013) 45-59.

[15] Z.P. Bažant, A. Steffens, Mathematical model for kinetics of alkali–silica reaction in concrete, Cement and Concrete Research, 30 (2000) 419-428.

[16] X. Hou, L.J. Struble, R.J. Kirkpatrick, Formation of ASR gel and the roles of C-S-H and portlandite, Cement and Concrete Research, 34 (2004) 1683-1696.

[17] A. Leemann, G. Le Saout, F. Winnefeld, D. Rentsch, B. Lothenbach, Alkali-silica reaction: the influence of calcium on silica dissolution and the formation of reaction products, Journal of the American Ceramic Society, 94 (2011) 1243-1249.
[18] D. Bulteel, E. Garcia-Diaz, C. Vernet, H. Zanni, Alkali–silica reaction: A method to quantify the reaction degree, Cement and Concrete Research, 32 (2002) 1199-1206.
[19] F. Iacopi, G. Beyer, Y. Travaly, C. Waldfried, D.M. Gage, R. Dauskardt, K. Houthoofd, P. Jacobs, P. Adriaensens, K. Schulze, Thermomechanical properties of thin organosilicate glass films treated with ultraviolet-assisted cure, Acta Materialia, 55 (2007) 1407-1414.
[20] X.-D. Cong, R.J. Kirkpatrick, S. Diamond, 29Si MAS NMR spectroscopic investigation of alkali silica reaction product gels, Cement and Concrete Research, 23 (1993) 13.
[21] R.K. Harris, E.K. Bahlmann, K. Metcalfe, E.G. Smith, Quantitative silicon-29 NMR investigations of highly concentrated high-ratio sodium silicate solutions, Magnetic Resonance in Chemistry, 31 (1993) 743-747.